Jewel Journal of Scientific Research (JJSR) 10(2): 325–335, 2025
©Federal University of Kashere-Nigeria (Print ISSN: 2384 – 6267, Online ISSN 2756-651X)
https://journals.fukashere.edu.ng/index.php/jjsr

Limitations of Pharmacophore Modeling for Intrinsically Disordered Plant Stress Proteins: A Case Study of DHN1 in *Zea mays*

***Ayinla, A.[1], Ibrahim, A.S[1]., Olayinka, B.U[2]., Opadokun, W.O[1]., Balogun, A., Lawal, A.R[4]., Koiki, A.O[1]., Kareem, I.[3] and Etejere, E.O[2].**

[1]Department of Biological Sciences, Al-Hikmah University, Ilorin
[2]Department of Plant Biology, University of Ilorin, Ilorin
[3]Department of Agronomy, University of Ilorin, Ilorin
[4]Department of Plant and Environmental Biology, Kwara State University Malete.
***Corresponding Author**: aayinla@alhikmah.edu.ng; +2347033906219

Abstract
Dehydrins are highly conserved drought-responsive proteins that protect plant cells, yet their molecular mode of action remains unclear. In maize (*Zea mays*), Dehydrin 1 (DHN1) is strongly induced by drought stress and is closely associated with stress-related metabolites including abscisic acid, (ABA), salicylic acid (SA), γ-aminobutyric acid (GABA), β-aminobutyric acid (BABA), and proline. This study assessed the structural feasibility of direct small-molecule binding to DHN1 using molecular docking and pharmacophore-based virtual screening. Disorder prediction confirmed that DHN1 is predominantly intrinsically disordered, with conserved K-segments involved in macromolecular interactions. Docking analyses revealed uniformly weak binding affinities (−2.033 to −2.561 kcal/mol), consistent with non-specific and transient surface contacts. Although pharmacophore modeling modestly improved docking scores, inconsistent binding geometries and poor RMSD convergence indicated a lack of true structural complementarity. These results support the classification of DHN1 as a non-ligand-binding protein that functions primarily through macromolecular stabilization and membrane association, highlighting the need to align computational approaches with protein structural properties in plant stress biology.

Keywords: Dehydrin 1 (DHN1), Plant-stress metabolites, Pharmacophore modeling, Intrinsically disordered proteins (IDPs), *Zea mays*

Received: 17th Sept, 2025 *Accepted:* 24th Nov, 2025 *Published Online:* 27th Dec 2025

Introduction

Drought stress is a major environmental constraint limiting crop productivity worldwide, primarily through its effects on cellular water balance, oxidative stress, and metabolic disruption (Gupta *et al*., 2020; Zhang *et al*., 2022). Under water-deficit conditions, plants activate a coordinated network of physiological and molecular responses aimed at preserving cellular integrity and ensuring survival. These responses include the accumulation of stress-protective proteins and a diverse array of small metabolites that function in signalling, osmotic adjustment, and redox homeostasis (Verslues *et al*., 2006). Among the most conserved drought-responsive proteins are dehydrins, a subclass of Late Embryogenesis Abundant (LEA) proteins. Dehydrins are intrinsically disordered proteins (IDPs) that lack stable tertiary structure but are highly flexible, enabling them to interact with multiple molecular targets. Functionally, they have been implicated in membrane stabilization, prevention of protein aggregation, ion binding, and protection against reactive oxygen species (Close, 1997; Hundertmark and Hincha, 2008; Hara, 2010;

Kosová *et al*., 2014). In maize (*Zea mays*), Dehydrin 1 (DHN1) is strongly induced under drought and osmotic stress and is thought to contribute to the maintenance of cellular homeostasis and macromolecular stability during dehydration (Cellier *et al*., 1998; Hara, 2010). In addition to protein-based mechanisms, several small metabolites including abscisic acid (ABA), salicylic acid (SA), γ-aminobutyric acid (GABA), β-aminobutyric acid (BABA), and proline play central roles in plant drought responses. These compounds act as stress signals, priming agents, osmoprotectants, and regulators of gene expression, and their accumulation is often temporally associated with dehydrin expression (Verslues and Sharma, 2010; Hilker *et al*., 2016; Balfagón *et al*., 2020). For instance, ABA is a key regulator of drought-induced gene expression, including dehydrin genes, while proline contributes to osmotic balance and stabilization of proteins and membranes under stress conditions (Cutler *et al*., 2010; Szabados and Savouré, 2010). Despite the well-established correlation between stress-related metabolites and dehydrin accumulation, it remains unclear whether these molecules directly interact with dehydrins at the structural level. This question is particularly important given the intrinsically disordered nature of dehydrins, which typically engage in transient, low-affinity, and dynamic interactions rather than forming stable ligand-binding pockets (Wright and Dyson, 2015; Uversky, 2019). Consequently, conventional assumptions about protein-ligand binding may not fully apply to these systems. This study therefore aimed to evaluate the structural feasibility of direct small-molecule binding to maize DHN1 using molecular docking and pharmacophore-based virtual screening approaches. Determining whether DHN1 can directly bind drought-associated metabolites is essential for clarifying its molecular mode of action and for informing the design of appropriate computational and experimental strategies to enhance drought tolerance in crops. Furthermore, insights gained from this study may have broader implications for crop improvement as a detailed understanding of DHN1 function and its potential interactions could inform the design of novel biostimulants or small-molecule modulators which could enhance drought resilience in crops such as maize considering the increasing global demand for food security under a constantly changing climatic conditions, (Lesk *et al*., 2022; Zhang *et al*., 2022).

Materials and Methods

Ligand Selection and Preparation

Five drought-associated small metabolites including abscisic acid (ABA), salicylic acid (SA), γ-aminobutyric acid (GABA), β-aminobutyric acid (BABA), and L-proline were selected based on their established roles in drought stress signaling and priming. Ligand structures were retrieved from the PubChem database in 2D SDF format and converted to PDB format using Open Babel. Ligand preparation involved geometry optimization, protonation at physiological pH (7.0), and energy minimization using the OPLS4 force field. Rotatable bonds were assigned, and partial charges were added prior to docking

Protein Preparation

The structures of the target proteins was retrieved from the Alphafold3 (https://alphafold.ebi.ac.uk/): Dehydring 1 (DHN1), the target protein for plant drought resistance (ID: AF-P12950-F1-v6). Protein preparation was performed using Maestro's Protein Preparation Wizard, which included addition of hydrogens, assignment of bond orders, optimization of hydrogen-bonding networks, and minimization with the OPLS4 force field. Missing side chains and loops was reconstructed, and appropriate charges and atom types was assigned to the target protein (Sahayarayan *et al*., 2021).

Structure-based Pharmacophore Modeling

Structure-based pharmacophore modeling was performed using the Pharmit web server to identify key interaction features governing ligand recognition within the dehydrin 1 (DHN1) K1 segment (residue 94-108) binding pocket of maize. In order to perform structure-based pharmacophore modeling; DHN1, the target protein for activation of

drought response signalling complexed was docked against each of the aforementioned drought associated small metabolites (abscisic acid (ABA), salicylic acid (SA), γ-aminobutyric acid (GABA), β-aminobutyric acid (BABA), and L-proline). Each of the docked protein and ligands was downloaded separately and saved in protein data bank (Pdb) format. Prepared receptor structures and ligands were inputted into Pharmit to derive pharmacophoric features directly from protein–ligand interactions. Interaction-based pharmacophoric features such as hydrogen bond donors, hydrogen bond acceptors, hydrophobic features, and negative ionizable features, corresponding to the key functional groups of each ligand involved in receptor binding were extracted from the ligand–protein complex. Exclusion volumes were generated within Pharmit to represent sterically inaccessible regions of the binding pocket, thereby improving pharmacophore selectivity and reducing false-positive matches. Inclusion volume was included to ensure that the generated models are roughly the same size and shape as the submitted ligand in order to avoid generating molecules too large and structurally inaccessible within the defined binding site. Afterwards, PubChem was selected as the chemical library for generating the pharmacophore models. The models pools were further subjected to energy minimizations. The first 20 models with the least minimized affinity for each of the ligands were downloaded and retrieved.

Receptor grid preparation

A protein grid (Glide grid) was constructed around the binding site of the target protein using Schrödinger's Receptor Grid Generation module. The binding site was defined by selecting the amino acid residues within the K1 segment. All amino acid residues within the active region was encompassed by an automatically generated cubic grid box (Owolade *et al*., 2025).

Molecular Docking

In order to evaluate the structural feasibility of direct ligand binding to the DHN1 protein in maize, molecular docking was carried out using the Glide module (Extra Precision, XP mode) in Schrödinger Maestro to evaluate ligand binding affinities within the active sites of the target proteins. The XP (extra precision) mode reduced intermediate conformations and optimized torsional refinement and sampling, thereby enhancing the accuracy of predicted binding poses and affinities within the protein's binding pocket (Omer *et al.*, 2022).

.

Results and Discussion

Intrinsic Disorder Defines DHN1 Functionality

Dehydrins are characterized by high structural plasticity and intrinsic disorder, properties that are essential for their biological function under stress (Uversky, 2013). DHN1 contains conserved K-segments that adopt amphipathic α-helices primarily during membrane association, enabling lipid stabilization and protection against dehydration-induced damage (Koag *et al*., 2009; Eriksson *et al*., 2011). These motifs are not known to form ligand-binding cavities, and their functional relevance lies in macromolecular and physicochemical interactions rather than molecular recognition.

The failure of pharmacophore-derived ligands to fit within DHN1 therefore reflects the true biophysical nature of the protein rather than a deficiency in ligand design. This finding provides computational support for the classification of DHN1 as a non-ligand-binding stress protein.

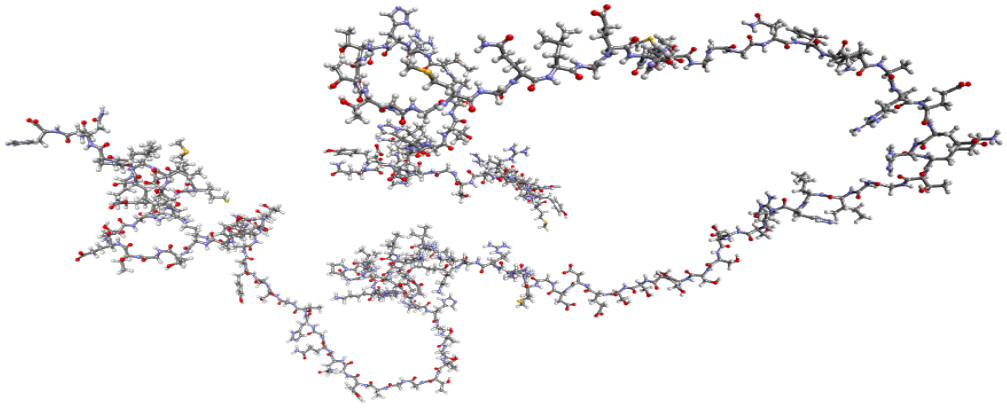

Figure 1: DHN1 Protein

Limited Binding Affinity of Stress-Associated Metabolites to DHN1

The binding affinities/docking scores of **drought-associated small metabolite** with drought resistance protein in maize, dehydrin 1 (DHN1) is shown in table 1. L-Proline showed highest binding energy within K1 segment (amino acid residue 94 – 108) with docking score of -2.561 kcal/mol while gamma-aminobutyric acid (GABA) has the lowest binding energy with the docking score of -2.033 kcal/mol. The initial docking analysis revealed uniformly weak binding affinities between DHN1 and the selected stress-associated metabolites, with docking scores ranging from −2.033 to −2.561 kcal/mol. These values are well below the threshold typically associated with stable and specific protein–ligand interactions and instead suggest transient, non-specific surface contacts (Kitchen *et al*., 2004). Although interactions were observed near the conserved K-segment region of DHN1, the low binding energies indicate that these contacts are unlikely to be biologically relevant.

Such weak interactions are consistent with previous computational observations involving intrinsically disordered proteins (IDPs), where docking algorithms often generate artificial binding poses on flexible protein surfaces that lack true ligand-recognition sites (Wright and Dyson, 2015).

Table 1: Docking scores for five drought-associated small metabolite in maize DHN1 protein

S/N	Compound Name	PubChem ID	Docking Score (kcal/mol)
1.	Gamma-aminobutyric acid (GABA)	119	-2.033
2.	Salicylic Acid	338	-2.076
3.	Abscisic Acid	5280896	-2.157
4.	3-Aminobutanoic acid/3-Aminobutyric acid/ beta-Aminobutyric acid (BABA)	10932	-2.171
5.	L-proline/Proline	145742	-2.561

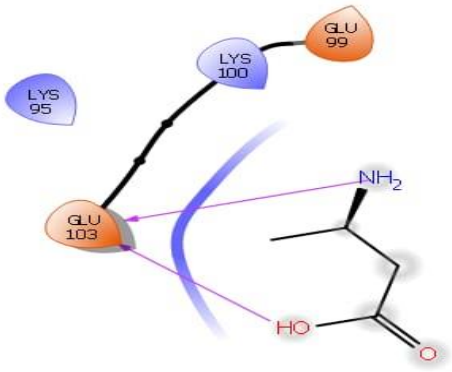

Figure 2: Docking between DHN1 protein and 3-Aminobutyric acid

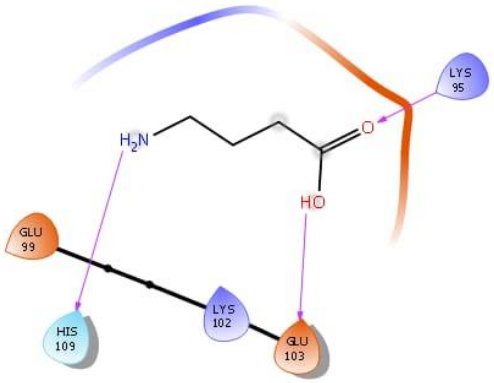

Figure 3: Docking between DHN1 protein and gama-Aminobutyric acid

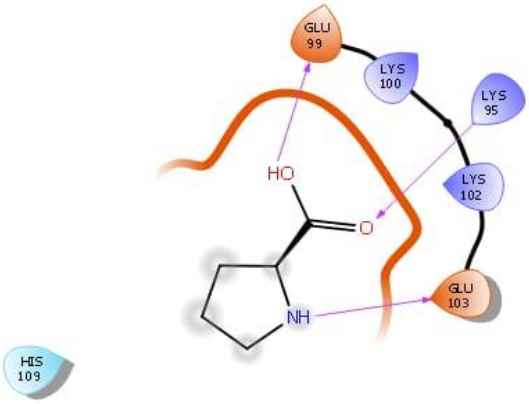

Figure 4: Docking between DHN1 protein and L-proline

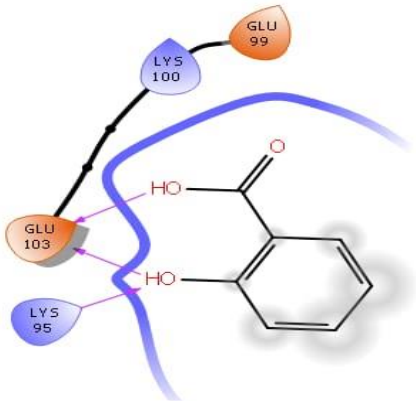

Figure 5: Docking between DHN1 protein and salicylic acid

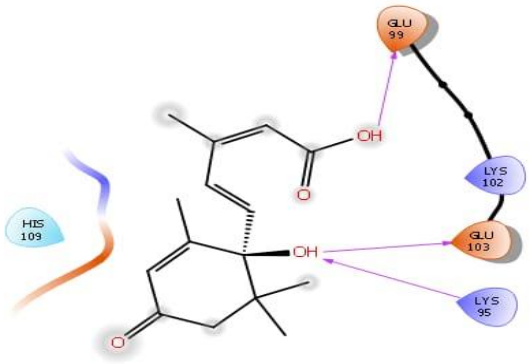

Figure 6: Interaction between DHN1 protein and Abscisic acid

Pharmacophore Modeling Improves Scores but Not Structural Compatibility. Structure-based pharmacophore modeling generated one hundred candidate compounds with moderately improved minimized affinities (up to approximately −4.07 kcal/mol). While these values represent an apparent improvement over the parent molecules, they remain within a weak binding range that is generally insufficient to support stable ligand–protein interactions. Contemporary studies on intrinsically disordered proteins (IDPs) indicate that small molecules typically interact with IDPs through low-affinity, transient, and non-specific contacts, rather than through well-defined, high-affinity binding pockets (Babu, 2023; Kulkarni *et al*., 2025). Consequently, the modest improvements observed in docking scores are unlikely to reflect biologically meaningful binding events. The absence of consistent low root-mean-square deviation (RMSD) values across the docked compounds further supports this result. In structured proteins, convergence toward low RMSD values is indicative of stable and reproducible binding conformations. However, IDPs exist as highly dynamic conformational ensembles, undergoing rapid interconversion between multiple structural states (Tompa, 2012; Wright and Dyson, 2015). As a result, docking simulations performed on such flexible systems frequently yield highly variable binding poses, depending on the conformational snapshot used as input (Tompa, 2012; Karatzas *et al*., 2025). Therefore, the improved docking scores observed here likely reflect increased molecular surface contact rather than genuine structural complementarity reinforcing the limitation of pharmacophore modeling when applied to proteins lacking persistent tertiary structure. These results highlight a fundamental limitation of structure-based pharmacophore modeling when applied to IDPs. Traditional pharmacophore approaches rely on the assumption of a stable three-dimensional binding site, an assumption that is not valid for proteins lacking persistent tertiary structure (Babu, 2023). Consequently, such methods may overestimate binding affinity and misinterpret non-specific interactions as meaningful ligand recognition (Karatzas *et al*., 2025; Kulkarni *et al*., 2025).

Table 1: Docking scores and structural compatibility between DHN1 protein and Pharmacophore Models generated from Gamma-aminobutyric acid

S/N	Models IUPAC Name	Model PubChem ID	Minimized Affinity	Minimized RMSD
1.	4-amino-4-hydroxycyclohexa-2,5-diene-1-carboxylic acid	146451675	-4.07004	0.9544
2.	1,3-dihydroxycyclopentane-1-carboxylic acid	19989925	-3.97955	1.12054
3.	1-amino-3-hydroxycyclopentane-1-carboxylic acid	67543287	-3.83893	1.28166
4.	6-aminobicyclo[3.1.0]hexane-3-carboxylic acid;hydrochloride	162422187	-3.73893	1.07178
5.	3-(hydroxyamino)-2,2-dimethylcyclopropane-1-carboxylic acid	163493362	-3.72547	0.96733
6.	4-amino-2-oxabicyclo[2.2.2]octane-1-carboxylic acid;hydrochloride	138584521	-3.61146	1.09276
7.	4-hydroxy-2-oxabicyclo[2.2.2]octane-1-carboxylic acid	138585161	-3.60421	1.05674
8.	trans-(1R,3S)-1-amino-3-hydroxycyclopentane-1-carboxylic acid;hydrochloride	136589191	-3.56474	1.21911
9.	cis-(1S,3S)-1-amino-3-hydroxycyclopentane-1-carboxylic acid	122218697	-3.53892	1.14285

10.	trans-(1S,3R)-1-amino-3-hydroxycyclopentane-1-carboxylic acid;hydrochloride	164662450	-3.53287	1.3448
11.	1-amino-3-hydroxycyclopentane-1-carboxylic acid;hydrochloride	165604526	-3.53286	1.34513
12.		154423017	-3.5328	1.34453
13.	4-hydroxycyclohex-3-ene-1-carboxylic acid	55302537	-3.4681	1.05641
14.	1,2,3,4,5,6-hexahydrocyclopenta[c]pyrrole-5-carboxylic acid	140192507	-3.45939	1.65344
15.	2-methyl-5-azaspiro[2.3]hexane-2-carboxylic acid	150916203	-3.38804	0.96879
16.	1-amino-3-hydroxycyclohexane-1-sulfonic acid	154466377	-3.38804	0.96879
17.	cis-(1S,3S)-3-(aminomethyl)-2,2-difluorocyclopropane-1-carboxylic acid	165763496	-3.38409	0.89595
18.	cis-(1S,3S)-3-amino-1-hydroxycyclopentane-1-carboxylic acid	57393686	-3.37372	1.84735
19.	3-amino-3-hydroxycyclohexane-1-sulfonic acid	145801163	-3.36584	2.51583
20.	trans-(1S,3R)-3-amino-1-fluorocyclopentane-1-carboxylic acid	97055189	-3.35612	1.40225

Table 2: Docking scores and structural compatibility between DHN1 protein and Pharmacophore Models generated from Salicylic acid

S/N	Models IUPAC Name	Model PubChem ID	Minimized Affinity	Minimized RMSD
1.	4-amino-3,5-dideuterio-2-hydroxybenzoic acid	11286589	-3.48635	1.49004
2.	potassium 4-carboxy-3-hydroxyphenolate	101199148	-3.48231	1.49307
3.	4-fluoro-2-hydroxybenzoic acid	67661	-3.48098	1.48808
4.	copper;bis(2,4-dihydroxybenzoic acid)	118856558	-3.47499	1.50031
5.	2-hydroxy-3,4-dimethyl-6-oxopyridine-1-carboxylic acid	70500640	-3.43985	0.5208
6.	(4-carboxy-3-pyridinyl)azanide;yttrium(3+)	20583204	-3.42094	1.46135
7.	3,4,5-trideuterio-2-deuteriooxybenzoic acid	131698722	-3.41823	1.38614
8.	4-amino-2,3,5-trideuterio-6-hydroxybenzoic acid	119081216	-3.4077	1.47635
9.	4-(trifluoromethylsulfanyl)phenol	3815158	-3.40238	1.51119
10.	copper bis((2-carboxyphenyl)azanide)	11967861	-3.40235	1.5107
11.	3-(3-methylphenyl)-3-oxopropanenitrile	143105	-3.39869	1.60942
12.	2-hydroxy-6-oxo-1H-pyridine-3-carboxylic acid	135526603	-3.38434	1.45356
13.	3-amino-2-hydroxy-5,6-dimethylbenzoic acid	84657754	-3.37179	0.67474
14.	3-hydroxy-1-methylpyridin-1-ium-4-carboxylic acid chloride	71719458	-3.36753	1.48359
15.	deuterio 2,3,4,5-tetradeuterio-6-deuteriooxybenzoate	71309006	-3.35772	1.31574
16.	2,3,4,5-tetradeuterio-6-deuteriooxybenzoic acid	155803953	-3.3537	1.34831
17.	3,5-dideuterio-2-hydroxybenzoic acid	102331052	-3.34918	1.38612
18.	3,4,5-trideuterio-2-hydroxybenzoic acid	140849591	-3.34918	1.38626
19.	4-deuterio-2-hydroxybenzoic acid	57607825	-3.34852	1.38397
20.	6-hydroxy(1,2,3,4,5,6-14C6)cyclohexa-1,3,5-triene-1-carboxylic acid	102602065	-3.3485	1.38398

Table 3: Docking scores and structural compatibility between DHN1 protein and Pharmacophore Models generated from Beta amino-butyric acid

S/N	Models IUPAC Name	Model PubChem ID	Minimized Affinity	Minimized RMSD
1.	1-[1-(2H-tetrazol-5-yl)cyclopropyl]ethanol	165723228	-3.1528	1.45665
2.	3-amino-2,2-difluorobicyclo[1.1.1]pentane-1-carboxylic acid	165887545	-3.11542	2.04624
3.	2-[(7S)-5-azaspiro[2.4]heptan-7-yl]acetic acid	125461906	-3.10628	1.48674
4.	(3-amino-2-methyl-4-oxoazetidin-1-yl)phosphonic acid	20153450	-3.07708	1.59528
5.	2-(2H-tetrazol-5-yl)butan-1-amine	69516624	-2.98236	3.50557
6.	2-(2H-tetrazol-5-yl)prop-2-en-1-amine	165785510	-2.86127	1.42217
7.	Ethyl-5-[(4-methoxycarbonylphenyl)methoxy]-2-phenyl-1-benzofuran-3-carboxylate	12313370	-2.85175	2.88575
8.	[2-(ethylamino)-2-methylpropyl] hydrogen sulfate	140281400	-2.8329	1.46583
9.	2-amino-3-(methylamino)pentanoic acid	116957309	-2.8282	1.55228
10.	2-(dimethylamino)-1-[(2S)-2-[4-[4-[(2S)-3-[2-(dimethylamino)acetyl]-3,9,10 triazatricyclo[5.2.1.02,6]deca-1(9),7-dien-2-yl]phenyl]phenyl]-3,9,10-triazatricyclo[5.2.1.02,6]deca-1(9),7-dien-3-yl]ethanone	57464986	-2.81817	1.52347
11.	(2S,3S)-2-amino-4-fluoro-3-hydroxy-3-methylbutanoic acid	45082004	-2.79533	3.15192
12.	(2S,3R)-2-amino-3-deuteriooxy-3-methylpentanoic acid	142347551	-2.75966	3.25348
13.	carbanide;methyl-(4-methylpyrrolidine-3-carbonyl)azanide;yttrium	57785760	-2.75803	1.89644
14.	O-[1-(2H-tetrazol-5-yl)ethyl]hydroxylamine	53867304	-2.73323	1.43029
15.	(1R)-N-methyl-1-(2H-tetrazol-5-yl)ethanamine	52213199	-2.72417	1.27286
16.	(2S)-2-chloro-3-hydroxybutanoic acid	87792783	-2.72133	2.93585
17.	2-chloro-3-hydroxybutanoic acid	542232	-2.71199	2.82972
18.	(2S,3R)-2-chloro-3-hydroxybutanoic acid	21586111	-2.71196	2.82977
19.	3-amino-2-fluorobicyclo[1.1.1]pentane-1-carboxylic acid	165683630	-2.69836	2.23926
20.	3-hydroxy-2-methylazetidine-1-carboxylic acid	158731457	-2.68999	1.24365

Table 4: Docking scores and structural compatibility between DHN1 protein and Pharmacophore Models generated from L-proline

S/N	Models IUPAC Name	Model PubChem ID	Minimized Affinity	Minimized RMSD
1.	2,3-dihydroxypiperidine-2-carboxylic acid	20058670	-3.36603	1.01365
2.	(3aR,6aR)-2,3,4,5,6,6a-hexahydro-1H-cyclopenta[c]pyrrole-3a-carboxylic acid	1519444	-3.3445	1.96145
3.	1-amino-1-hydroxyprop-2-ene-1-sulfonic acid	90301100	-3.3389	3.14944
4.	[(1S,2R)-1-amino-2-methylcyclopropyl]phosphonic acid	132538899	-3.24539	0.50479
5.	3-amino-3-(2H-tetrazol-5-yl)cyclobutan-1-ol	165782150	-3.18878	1.05206
6.	(2R)-1,2-dihydroxypiperidine-2-carboxylic acid	141142874	-3.18813	0.72048
7.	(1S,6R)-1,6-dihydroxycyclohexa-2,4-diene-1-carboxylic acid;methyl (1S,6R)-1,6-dihydroxycyclohexa-2,4-diene-1-carboxylate;molecular iodine;triiodide	158058106	-3.18135	0.76123
8.	(1-amino-1-hydroxyprop-2-enyl)phosphonic acid	87724819	-3.04553	2.3103
9.	1-(2H-tetrazol-5-yl)cyclopentan-1-amine	54594012	-3.0253	1.23185
10.	(1S)-1-amino-2-hydroxycyclohexane-1-carboxylic acid	15813568	-2.99317	0.831
11.	6-amino-5-hydroxycyclohex-2-ene-1-carboxylic acid	57010842	-2.98706	1.00919
12.	2,2-dimethyl-1-(2H-tetrazol-5-yl)cyclopropan-1-amine	165717066	-2.96171	1.19083
13.	sodium 1-hydroxy-2,2-dimethylpropane-1-sulfonate	23663696	-2.95151	3.39048
14.	[5,7,8-trifluoro-2-(trifluoromethyl)quinolin-4-yl]hydrazine	62812423	-2.94925	0.69311
15.	N'-quinazolin-4-ylacetohydrazide	2543146	-2.94743	2.73798
16.	(1S)-1,6-dihydroxycyclohexa-2,4-diene-1-carboxylic acid	126660594	-2.93984	0.87771
17.	(1S,6R)-1,6-dihydroxycyclohex-2-ene-1-carboxylic acid	134232391	-2.93376	0.80654
18.	1,1-diaminoprop-2-ene-1-sulfonic acid	88316246	-2.92909	3.04266
19.	3-amino-3-(2H-tetrazol-5-yl)cyclobutan-1-ol	165782150	-2.9261	1.59438
20.	2-[(1R,5S)-5-hydroxycyclopent-2-en-1-yl]acetic acid	12813247	-2.9228	1.72324

Biological Context of Stress Metabolites

ABA, SA, GABA, BABA, and proline are well-established mediators of drought stress responses; however, their primary roles involve signaling, transcriptional regulation, and metabolic adjustment rather than direct protein binding (Zhang *et al*., 2006; Verslues *et al*., 2006). ABA regulates dehydrin expression through ABA-responsive transcription factors, while proline contributes to osmotic balance and redox buffering (Szabados and Savouré, 2010). GABA and BABA function as stress priming agents that enhance downstream defense responses without acting as direct ligands (Hilker *et al*., 2016). The absence of stable binding between these metabolites and DHN1 is therefore consistent with their established modes of action and supports a regulatory rather than ligand-mediated relationship. This study highlights an important methodological consideration in plant computational biology where ligand-based modeling approaches are not universally applicable to all stress-responsive proteins. For intrinsically disordered proteins such as DHN1, alternative strategies such as molecular dynamics simulations, disorder analysis, protein-membrane interaction modeling, and protein-protein interaction studies could be more appropriate for capturing functional mechanisms (Babu *et al*., 2011). Most importantly, the present findings should be

viewed as a positive mechanistic clarification, demonstrating that DHN1 does not operate via small-molecule binding. This insight can help redirect future in silico and experimental efforts toward biologically relevant targets, such as ABA receptors or transcriptional regulators, where ligand-binding mechanisms are structurally plausible.

Conclusion

In conclusion, the inability of pharmacophore-derived compounds to establish stable interactions with maize DHN1 reflects the intrinsically disordered and non-ligand-binding nature of the protein. DHN1 may likely confers drought tolerance through macromolecular stabilization, membrane association, and hydration shell formation rather than direct interaction with stress-related metabolites. These findings underscore the importance of aligning computational approaches with protein structural properties and provide a refined framework for future modeling of plant stress proteins.

References

Babu, M. M. (2016). The contribution of intrinsically disordered regions to protein function, cellular complexity, and human disease. *Biochemical Society Transactions*, 44(5): 1185-1200.

Balfagón, D., Sengupta, S., Gómez-Cadenas, A., and Fritschi, F. B. (2020). Jasmonic acid is required for plant acclimation to a combination of high light and heat stress. *Plant Physiology*, 181(4): 1668–1682.

Cellier, F., Conejero, G., Breitler, J. C., and Casse, F. (1998). Molecular and physiological responses to water deficit in drought-tolerant and drought-sensitive lines of sunflower Accumulation of dehydrin transcripts correlates with tolerance. *Plant Physiology*, 116(1): 319–328. https://doi.org/10.1104/pp.116.1.319

Close, T. J. (1997). Dehydrins: A commonality in the response of plants to dehydration and low temperature. *Physiologia Plantarum*, 100(2): 291–296. https://doi.org/10.1111/j.1399-3054.1997.tb04785.x

Cutler, S. R., Rodriguez, P. L., Finkelstein, R. R., and Abrams, S. R. (2010). Abscisic acid: Emergence of a core signaling network. *Annual Review of Plant Biology*, 61: 651–679.

Eriksson, S. K., Kutzer, M., Procek, J., Gröbner, G., and Harryson, P. (2011). Tunable membrane binding of the intrinsically disordered dehydrin Lti30, a cold-induced plant stress protein. *The Plant Cell*, 23(6): 2391–2404. https://doi.org/10.1105/tpc.110.081091

Gupta, A., Rico-Medina, A., and Caño-Delgado, A. I. (2020). The physiology of plant responses to drought. *Science*, 368(6488): 266–269.

Hara, M. (2010). The multifunctionality of dehydrins: An overview. *Plant Signaling & Behavior*, 5(5): 503–508. https://doi.org/10.4161/psb.5.5.10930

Hilker, M., Schwachtje, J., Baier, M., Balazadeh, S., Bäurle, I., Geiselhardt, S. and Kopka, J. (2016). Priming and memory of stress responses in organisms lacking a nervous system. *Biological Reviews*, 91(4): 1114–1133. https://doi.org/10.1111/brv.12215

Hundertmark, M., and Hincha, D. K. (2008). LEA (late embryogenesis abundant) proteins and their encoding genes in *Arabidopsis thaliana*. *BMC Genomics, 9*, 118. https://doi.org/10.1186/1471-2164-9-118

Karatzas, P., Brotzakis, Z. F., and Sarimveis, H. (2025). Small Molecules Targeting the Structural Dynamics of AR-V7 Partially Disordered Proteins Using Deep Ensemble Docking. *Journal of Chemical Theory and Computation*, 21(9): 4898-4909.

Kitchen, D. B., Decornez, H., Furr, J. R., and Bajorath, J. (2004). Docking and scoring in virtual screening for drug discovery: Methods and applications. *Nature Reviews Drug Discovery*, 3(11): 935–949. https://doi.org/10.1038/nrd1549

Koag, M. C., Wilkens, S., Fenton, R. D., Resnik, J., Vo, E., and Close, T. J. (2009). The K-segment of maize DHN1 mediates binding to anionic phospholipid vesicles and concomitant structural changes. *Plant*

Physiology, 150(3): 1503–1514. https://doi.org/10.1104/pp.109.136697

Kosová, K., Vítámvás, P., and Prášil, I. T. (2014). Proteomics of stress responses in wheat and barley—search for potential protein markers of stress tolerance. *Frontiers in plant science*, 5(711): 1-14.

Kulkarni, P., Porter, L., Chou, T. F., Chong, S., Chiti, F., Schafer, J. W., and Salgia, R. (2025). Evolving concepts of the protein universe. *Iscience*, 28(112012): 1-13.

Lesk, C., Rowhani, P., and Ramankutty, N. (2016). Influence of extreme weather disasters on global crop production. 529(7584): 84-87.

Omer, S. E., Ibrahim, T. M., Krar, O. A., Ali, A. M., Makki, A. A., Ibraheem, W., and Alzain, A. A. (2022). Drug repurposing for SARS-CoV-2 main protease: Molecular docking and molecular dynamics investigations. *Biochemistry and Biophysics Reports*, 29: 101225. https://doi.org/10.1016/j.bbrep.2022.101225

Omer, S., Ali, M., and Khan, A. (2022). Advances in molecular docking methods and their application in plant stress biology. *Journal of Biomolecular Structure and Dynamics*, 40(15): 6890–6904. https://doi.org/10.1080/07391102.2021.1904872

Owolade, A. J.-J., Bodun, D., Akinbi, E. O., Oni, S. A., Omojuyigbe, J. O., Olatunji, T. W., Sylvanus, A. C., and Oke, A. E. (2025). Computational design of novel diphtheria toxin inhibitors using natural products-based drug discovery. *The Microbe*, 7: 100359. https://doi.org/10.1016/j.microb.2025.100359

Owolade, O. F., Aderibigbe, T. A., and Adeyemi, T. O. (2025). Structure-based virtual screening of stress-responsive proteins in crops under abiotic stress. *Computational Biology and Chemistry*, 104: 107870.

Sahayarayan, J. J., Rajan, K. S., Vidhyavathi, R., Nachiappan, M., Prabhu, D., Alfarraj, S., Arokiyaraj, S., and Daniel, A. N. (2021). In-silico protein-ligand docking studies against the estrogen protein of breast cancer using pharmacophore based virtual screening approaches. *Saudi Journal of Biological Sciences*, 28(1): 400–407. https://doi.org/10.1016/j.sjbs.2020.10.023

Sahayarayan, J. J., Soundararajan, P., and Chung, S. Y. (2021). Computational strategies in protein preparation and molecular docking: Advances and applications. *Journal of Molecular Modeling*, 27: 274. https://doi.org/10.1007/s00894-021-04868-4

Szabados, L., and Savouré, A. (2010). Proline: A multifunctional amino acid. *Trends in Plant Science*, 15(2): 89–97.

Tompa, P. (2012). Intrinsically disordered proteins: A 10-year recap. *Trends in Biochemical Sciences*, 37(12): 509–516.

Uversky, V. N. (2013). Intrinsically disordered proteins and their "mysterious" (meta)physics. *Frontiers in Physics*, 1: 1–18. https://doi.org/10.3389/fphy.2013.00002

Uversky, V. N. (2019). Intrinsically disordered proteins and their "mysterious" (meta)physics. *Frontiers in Physics*, 7(10): 1-18.

Verslues, P. E., and Sharma, S. (2010). Proline metabolism and its implications for plant–environment interaction. *The Arabidopsis Book*, 8: 1-23. https://doi.org/10.1199/tab.0140

Verslues, P. E., Agarwal, M., Katiyar-Agarwal, S., Zhu, J., and Zhu, J. K. (2006). Methods and concepts in quantifying resistance to drought, salt and freezing, abiotic stresses that affect plant water status. *The Plant Journal*, 45(4): 523-539.

Wright, P. E., and Dyson, H. J. (2015). Intrinsically disordered proteins in cellular signalling and regulation. *Nature Reviews Molecular Cell Biology*, 16(1): 18–29. https://doi.org/10.1038/nrm3920

Zhang, H., Zhu, J., Gong, Z., and Zhu, J. K. (2022). Abiotic stress responses in plants. *Nature Reviews Genetics*, 23(2): 104-119.